PERGAMON

International Journal of Solids and Structures 37 (2000) 6321–6341

INTERNATIONAL JOURNAL OF SOLIDS and STRUCTURES

www.elsevier.com/locate/ijsolstr

The crush behaviour of Rohacell-51WF structural foam

Q.M. Li, R.A.W. Mines*, R.S. Birch

Impact Research Centre, Department of Engineering, University of Liverpool, Brownlow Street, Liverpool L69 3GH, UK

Received 12 February 1999; in revised form 8 September 1999

Abstract

Various mechanical behaviours of Rohacell-51WF foam are studied in the present paper. Uniaxial tension and compression, and pure shear properties are obtained using standard test techniques. A hydrostatic test rig was designed to conduct hydrostatic compressive tests on the foam. These material tests give basic mechanical properties of the studied foam. Transverse shear effects on the compressive behaviour of the foam are studied by developing a shear-compression test technique. Deformation and failure features during foam crushing are discussed according to experimental evidence.

Keywords: Foam structures; Mechanical property; Failure

1. Introduction

Foam materials have a cellular structure with a three-dimensional array of cells and they are being used increasingly in engineering. Their microscopic cellular structure determines their superior performance as an energy absorbing material and as a core material in sandwich panels. However, their mechanical behaviours are complex due to their cellular structure. More material tests are required to determine their mechanical properties for structural design and numerical simulation purposes. Currently, the standard tests on mechanical properties of foam material include uniaxial tensile (ASTM C297-61, 1984), uniaxial compressive (ASTM D3574-91; ASTM C365-57) and pure shear (ASTM C273-61) tests. Foam behaviours under hydrostatic compression are also essential for numerical simulations and the corresponding experimental techniques have been developed (Triantafillou et al., 1989; Akfert, 1994; Maji et al., 1995).

In order to understand the mechanical behaviours of foam materials in the general loading case, experimental and theoretical studies have been conducted for a variety of loading paths. Yield and

* Corresponding author. Tel.: +44-0151-794-4819; fax: +44-0151-794-4848.
E-mail address: mines@mechnet.liv.ac.uk (R.A.W. Mines).

0020-7683/00/$ - see front matter
PII: S0020-7683(99)00277-2

failure surfaces of various foams have been presented (for example, Shaw and Sata, 1966; Triantafillou et al., 1989; Theocaris, 1992; Maji et al., 1995; Neilsen et al., 1995; Zhang et al., 1997; Mines et al., 1998), based on experimental results and constitutive models. Microscopic mechanics of cellular materials has been introduced by Gibson and Ashby (1988) to relate macroscopic behaviour to cell-wall properties and geometric constructions of the foam. Although considerable work has been done on foam materials, there still exist great difficulties in fully understanding foam behaviours in complex loading cases because of the complexity of foam structures.

The Rohacell polymethacrylimide series foams have application potential in aerospace and aircraft structures. The impact behaviour of Rohacell foams and sandwich panel constructions with the Rohacell foam have been studied in various ways (Bernard and Lagace, 1987; Tsang and Dugundji, 1990; Akay and Hanna, 1990; Wu and Sun, 1996). Foam structure and its influence on macroscopic properties of Rohacell foams were analysed by Chen et al. (1994) and Chen and Lakes (1995) using the microscopic formulations introduced by Gibson and Ashby (1988). The compressive process of Rohacell-51WF foam was studied by Li and Mines (1999), where the strain measures of a progressively crushing foam were formulated.

The purpose of this paper is to study the mechanical behaviour of Rohacell-51WF foam under various loading conditions. In addition to the basic material tests, i.e., uniaxial tensile, uniaxial compressive and pure shear tests, hydrostatic compressive and shear compressive tests were designed and conducted. Hydrostatic compressive results are necessary in foam material models (Bilkhu et al., 1993; Maji et al., 1995; Zhang et al., 1997), whilst shear compressive stress states may occur in sandwich panels subjected to mass impact (Mines et al., 1994; Mines and Jones, 1995; Mines, 1998). The effects of pre-compressive crushing damage on tensile properties of foam material were also studied.

2. Basic mechanical properties of Rohacell-51WF foam

2.1. Foam description

The studied foam is Rohacell-51WF from Roehm Ltd (Roehm, 1998). The foam is a closed cell rigid PMI (polymethacrylimide) foam. The microscopic structure of Rohacell-51WF foam is shown in Fig. 1. The characteristic cell-wall size and cell-wall thickness are $l = 0.3$ mm and $t = 12.0$ μm, respectively.

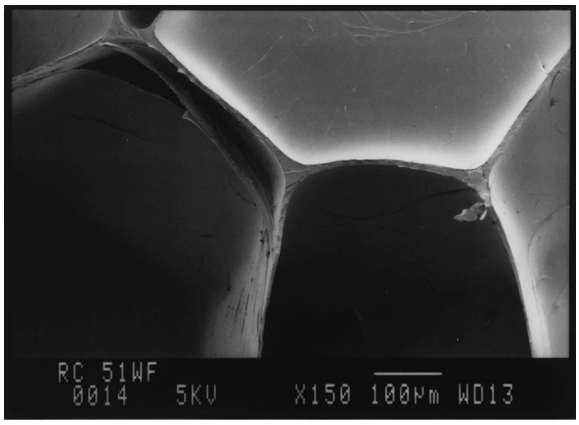

Fig. 1. Microstructure of Rohacell-51 WF foam (courtesy of Roehm Ltd.).

Table 1
Rohacell 51 WF data from manufacturer

Density (kg m^{-3})	52.0
Compressive strength (MPa)	0.8
Tensile strength (MPa)	1.6
Flexural strength (MPa)	1.6
Shear strength (MPa)	0.8
Tensile modulus (MPa)	75.0
Shear modulus (MPa)	19.0
Elongation at break (%)	3.0

Manufacturer's data for foam mechanical properties are given in Table 1. Mechanical properties of the PMI cell-wall material are shown in Table 2 according to Chen and Lakes (1995).

The tested specimens were cut from 10 and 20 mm thick panels of foam supplied by Roehm with a full certificate of conformity. Specimens were tested in the as supplied condition. It should be noted that the foam can be heat treated (48 h at 180°C) in order to improve its creep performance (Roehm, 1998).

2.2. Uniaxial compressive test

The compressive process of Rohacell-51WF foam has been described by Li and Mines (1999), which has the general feature of localised progressive collapse. Typical engineering compressive stress–strain curves tested at three mutually perpendicular directions of the foam are shown in Fig. 2, and it can be seen that the stress–strain curves are similar in these three directions. Stress–strain curves in other directions have not been measured and therefore, the anisotropic level of the foam cannot be guaranteed. However, the micro-mechanical model developed by Chen and Lakes (1995) suggests a relatively low level of anisotropy in non-principal directions. In Fig. 2, a non-linear feature is observed in the elastic range of Rohacell-51WF foam before yielding, which is due to the combined influence from material non-linearity and seating effects on the compressive platens. Another possible source of non-linearity is internal air pressure for closed cell foams (Gibson and Ashby, 1988). But, as E for the foam here is 75 MPa and as atmospheric air pressure is 0.1 MPa, then internal air pressure contribution is negligible.

The plateau range of crushable foam in compression, caused by cell-wall collapse, is the primary concern for crashworthiness applications. The cell-wall collapse in compression could be one of cell-wall buckling, cell-wall breaking and the formation of plastic hinges in the cell wall, or their combinations (Gibson and Ashby, 1988). The general feature of this process is that the capability of the cell wall to sustain the compressive force after collapse is smaller than the critical value at which the collapse is initiated. This leads to a progressive collapse mechanism and the macroscopic compressive stress stays as a constant (constant plateau stress) without strain hardening. The deformations in the foam are not uniform during this process and this has been studied by Li and Mines (1999). After all cells are locked

Table 2
Material properties of PMI[a]

Material	E_s (MPa)	σ_{ys} (MPa)	ρ_s (kg m^{-3})	ρ^*/ρ_s
PMI	5200.0	90.0	1200.0	0.043

[a] E_s: compressive Youngs' modulus; σ_{ys}: compressive yield stress; ρ_s: material density of PMI; ρ^*/ρ_s: relative density of foam material, where ρ^* is the density of Rohacell-51 WF foam.

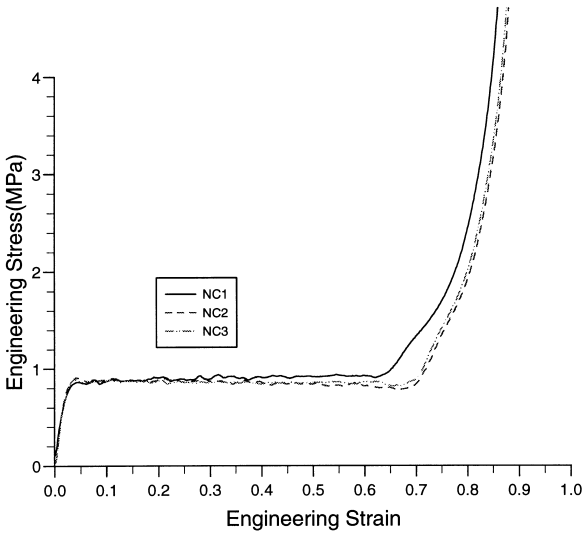

Fig. 2. Typical compressive engineering stress–engineering strain curves in three mutually perpendicular directions.

up (or densification has initiated), foam cells start to interact with each other, and the compressive stress will increase with further increase of compressive strain. The deformation across the specimen gauge length becomes uniform.

Basic mechanical properties in compression are given in Table 3. These uniaxial compressive material tests were conducted on a standard INSTRON 50 kN servo-hydraulic machine at a quasi-static loading rate of 1 mm/min, which gives an engineering strain rate of 8.3×10^{-4} s^{-1}, according to standards ASTM D3574-91 and ASTM C365-57. Stress was derived from the load cell and engineering strain was derived from cross head displacement. If the Young's modulus is defined by the tangent of the secant line from the origin to the yield stress point, the average Young's modulus is 22 MPa for quasi-static loading, which is much less than the tensile modulus from tensile test (Table 5) and the manufacturer's data. This is caused by using the uncompensated cross-head displacement to obtain engineering strain and possible seating effects. Thus, it is recommended to use tensile modulus as the compressive modulus because they normally should have similar values (Neilsen et al., 1995). As there is negligible lateral permanent deformation during compressive crushing, it is reasonable to assume that the plastic Poisson's ratio in the plateau range is zero. There are no obvious differences in compressive mechanical behaviours between the 10 and 20 mm thickness foams.

Strain rate effects on both, compressive yield stress and lock-up strain are shown in Figs. 3 and 4 for rates of 10^{-4}–10^{2} s^{-1}. The compressive tests up to 10^{0} s^{-1} were conducted on the INSTRON machine and the high rate tests were conducted on an ESH hydraulic dynamic test machine. The following equations are proposed to describe the strain rate dependence of yield stress

Table 3
Compressive properties of Rohacell-51 WF foam[a]

E (MPa)	σ_y (MPa)	ε_y (%)	ε_L (%)
22.0	0.8	4.6	68.9

[a] E: compressive Youngs' modulus; σ_y: compressive yield stress; ε_y: compressive yield strain; ε_L: lock-up strain.

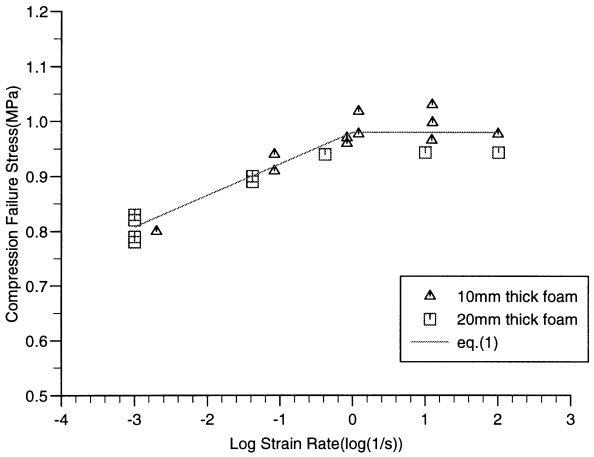

Fig. 3. Yield stress vs. log strain rate for compressive tests.

$$\sigma_y = \sigma_{ry} + A \log\left(\frac{\dot{\varepsilon}}{\dot{\varepsilon}_r}\right), \quad \text{for } 10^{-3}\ \text{s}^{-1} < \dot{\varepsilon} < 10^{0}\ \text{s}^{-1},$$

$$\sigma_y = 0.98\ \text{MPa}, \quad \text{for } 10^{0}\ \text{s}^{-1} < \dot{\varepsilon} < 10^{2}\ \text{s}^{-1} \tag{1}$$

where, $\dot{\varepsilon}_r = 10^{-3}\ \text{s}^{-1}$ is the reference strain rate, $\sigma_{ry} = 0.81$ MPa is the yield stress at $\dot{\varepsilon}_r$ and $A = 0.056$ MPa is a constant determined from the experimental curve. Fig. 4 shows some rate dependence in lock-up strain above the $10^0\ \text{s}^{-1}$ strain rate.

2.3. Hydrostatic compressive test

Many numerical foam material models require hydrostatic compressive results to determine

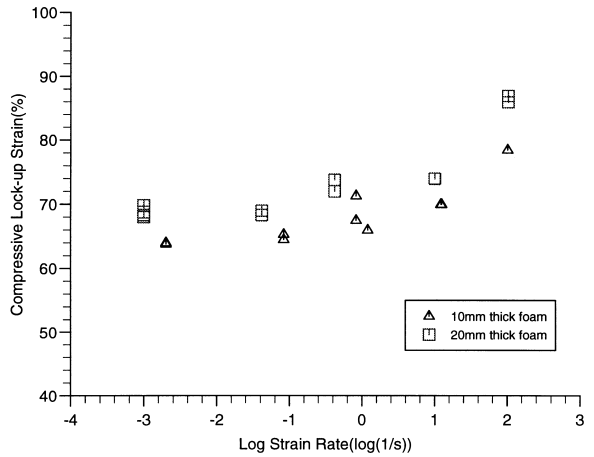

Fig. 4. Lock-up strain vs. log strain rate for compressive tests.

parameters and give hardening laws within the model (Bilkhu et al., 1993; Maji et al., 1995; Zhang et al., 1997). A test rig developed at UMIST (Akfert, 1994) was taken as the basic idea and a special rig, shown in Fig. 5, was designed and built to conduct the hydrostatic compressive foam test. The specimen is in the form of a 40 mm diameter cylinder of thickness 20 mm. The specimen is then surrounded by a Latex tube with the aid of 'O' rings. The compressive medium is water, and the water is stirred to remove air bubbles. The piston is then positioned and pushed in until all trapped air has escaped. The assembly is then placed onto the INSTRON 50 kN servo-hydraulic test machine and compressed. The pressure in the water and the displacement of the piston are measured.

The change in volume of the foam, ΔV, is given by

$$\Delta V = \pi R^2 x \tag{2}$$

where R is the radius of the piston, and x is the piston displacement. The volumetric strain ε_{vol} is then given by

$$\varepsilon_{\text{vol}} = \log\left[1 - \frac{\Delta V}{V_0}\right] \tag{3}$$

where V_0 is the original volume of the foam (Akfert, 1994). The relationships between pressure and volumetric strain for three tests are shown in Fig. 6(a). The average values from three tests for hydrostatic compression test are summarised in Table 4. Fig. 6(b) shows the specimen after test. The figure corresponds to very large strains, i.e. $\varepsilon_{\text{vol}} = 2$. It is proposed that the experiment condition is more

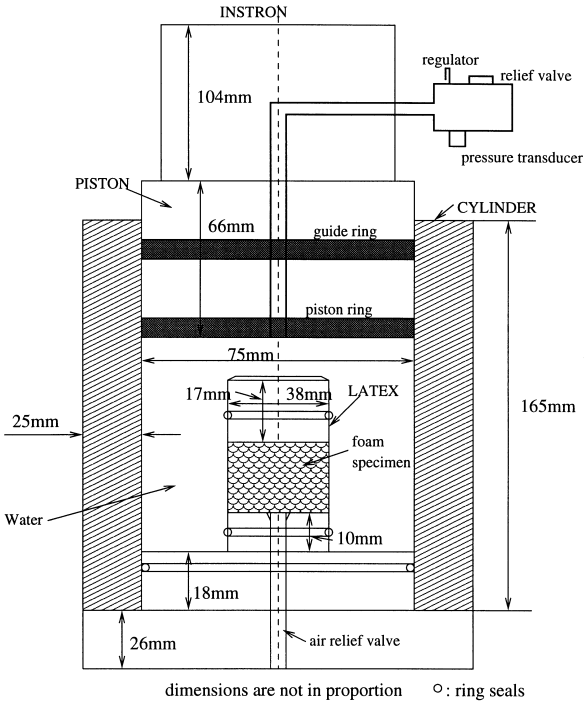

Fig. 5. Layout of hydrostatic test rig.

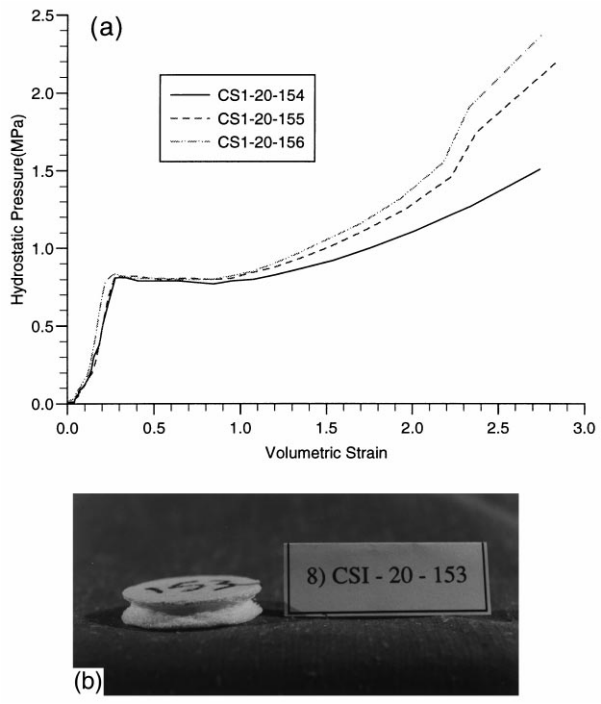

Fig. 6. (a) Hydrostatic pressure vs. volumetric strain data for hydrostatic tests (b) Foam specimen after hydrostatic compressive test.

closely associated with hydrostatic compression at smaller strains. An effort was made in the tests to lubricate the surfaces between the foam specimen and end caps.

2.4. Pure shear test

Core shear in sandwich panels has been realised as an important failure mode, which may further lead to structural failures. The pure shear tests were conducted according to standard ASTM C273. The specimen dimensions were $240 \times 40 \times 20$ mm. They were cut out of the 20 mm thick panel and bonded to the shear test platens using an epoxy adhesive. The tension version of the shear test was initially tried, but failure occurred along the load line invalidating the test. Hence, the compressive version of the test was used. A typical shear stress–shear strain curve is shown in Fig. 7, and the failed specimen is shown in Fig. 8. Shear strain was derived using a linear variable differential transformer (LVDT) which measured the relative displacement between the two platens. The foam is fairly brittle showing little crushing after failure. Failure occurs at 45° direction of the shear direction, which implies that the

Table 4
Hydrostatic compressive properties of Rohacell-51WF foam[a]

P_y (MPa)	$-\varepsilon_{vol}^{y}$ (%)	P_L (MPa)	$-\varepsilon_{vol}^{L}$ (%)
0.82	25.4	0.79	84.1

[a] P_y, P_L: yield and lock-up pressures; $-\varepsilon_{vol}^{y}$, $-\varepsilon_{vol}^{L}$: yield and lock-up volumetric strains.

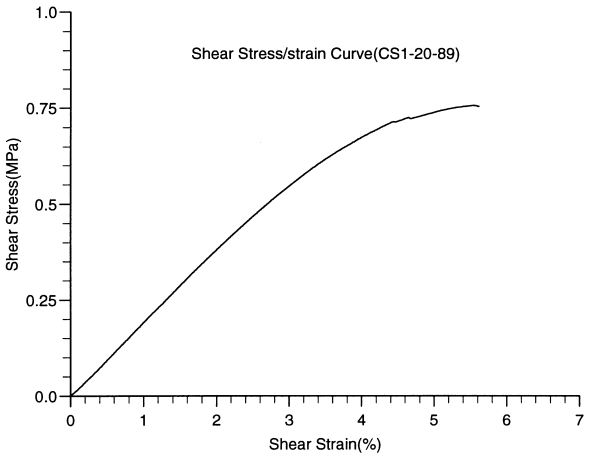

Fig. 7. A typical shear stress–shear strain curve for the pure shear test.

maximum tensile stress controls the failure. Shear properties of Rohacell-51WF foam are summarised in Table 5, which are comparable with manufacturer's data in Table 1. Note that τ_f and γ_f correspond to total failure of the foam, and values given are the average from three tests.

Variations of shear failure stress and failure strain with log strain rate from $10^{-3.5}$ to 10^{0} s^{-1} are shown in Figs. 9 and 10. It seems that shear failure strain is independent of strain rate within this range. However, shear failure stress starts to fall from $10^{-1.4}$ s^{-1}.

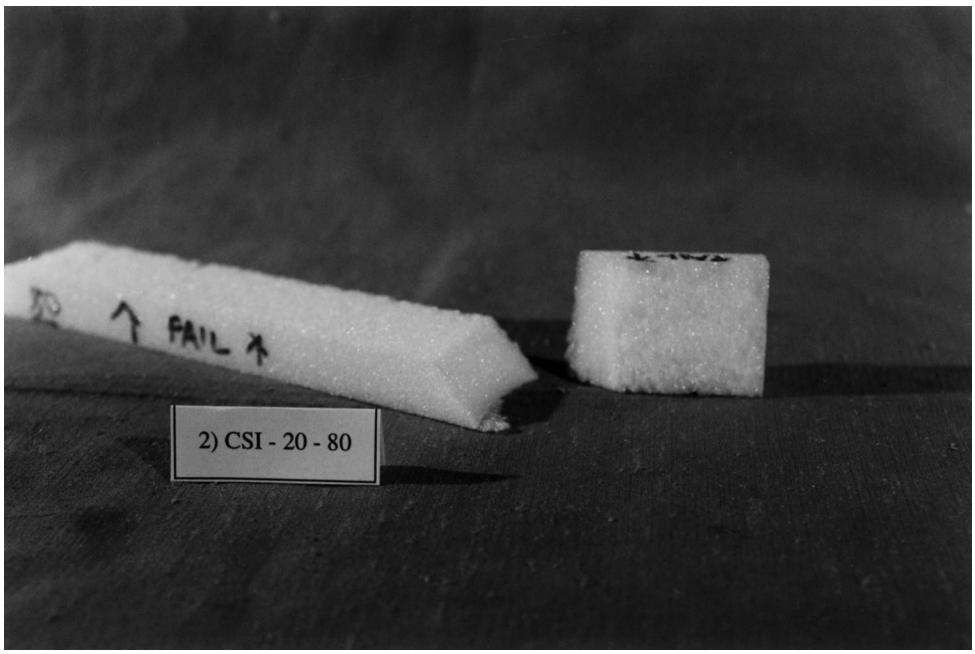

Fig. 8. Photograph of failed specimen in pure shear (failure occurs at 45°).

Table 5
Shear and tension properties of Rohacell-51 WF foam[a]

E (MPa)	G (MPa)	γ_f (%)	τ_f (MPa)	ε_f (%)	σ_f (MPa)
88.0	19.1	5.32	0.76	1.98	1.50

[a] E, G: tensile and shear modulus; ε_f, γ_f: tensile and shear failure strains; σ_f, τ_f: tensile and shear failure strength.

2.5. Uniaxial tensile test

Flatwise tensile tests were conducted on the INSTRON test machine according to ASTM C297-61. The loading rig had two perpendicular axes of rotation in order to eliminate bending stresses in the specimen due to misalignment. Specimens were cut out of both 10 and 20 mm thickness foam panels. The loading speed was 0.05 mm/min, which offers a strain rate below 10^{-4} s^{-1} for both thickness foams.

The tensile test results for 10 mm thickness foam are presented in Fig. 11. The average values of tensile properties for both 10 and 20 mm thickness foams are given in Table 5. As in the case of shear loading, σ_f and ε_f correspond to total failure of the foam and values given here are the averages from seven tests. There is a slight difference in tensile properties between 10 and 20 mm Rohacell-51WF foams. However, average values in Table 5 are comparable with manufacturer's data in Table 1.

As mentioned previously, the anisotropic properties of the foam have not been quantified here. Gibson and Ashby (1988) show that in general, low density foams tend to be more anisotropic than high density foams. However, the microstructure of the foam considered here suggests a relatively low level of anisotropy (Chen and Lakes, 1995). When the relationship between shear and tensile/compressive modulus for an isotropic material is used, i.e.,

$$\nu = \frac{E}{2G} - 1, \tag{4}$$

then $\nu = -0.42$ from compressive and shear moduli and $\nu > 1.1$ from tensile and shear moduli. Thus, the legitimacy of Eq. (4) and an isotropic material model for the studied foam is questionable. Gibson and Ashby (1988) found that the Poisson's ratio for both open and closed cell foams is 1/3 when Eq. (4)

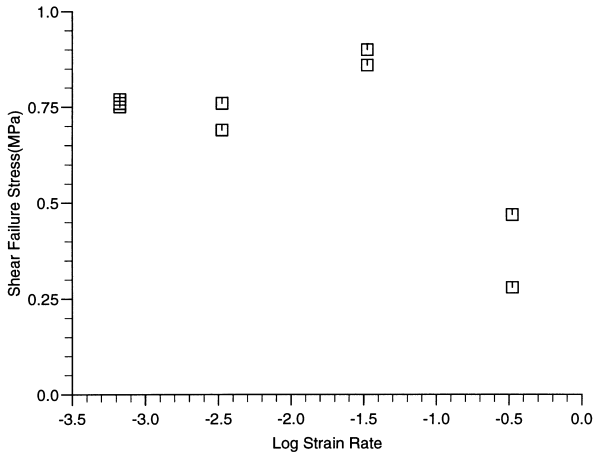

Fig. 9. Shear failure stress vs. log strain rate for pure shear test.

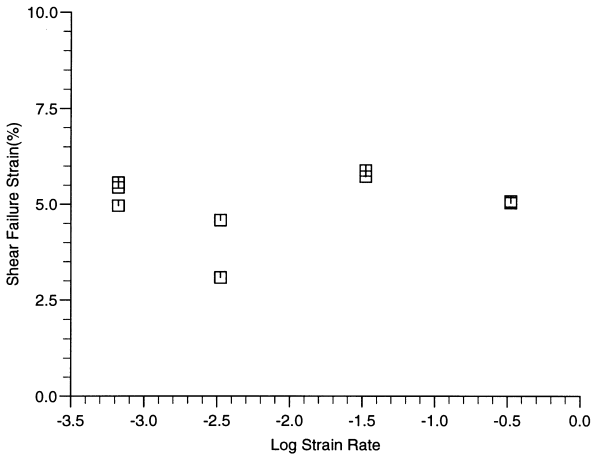

Fig. 10. Shear failure strain vs. log strain rate for pure shear test.

is used. They also admitted a larger scatter in the data for Poisson's ratio although their average is approaching a value of 1/3. Triantafillou and Gibson (1990) also indicated the inconsistency in the relationship between bulk modulus, Young's modulus and Poisson's ratio when the isotropic formula is used.

It has been shown by Triantafillou et al. (1989) that the uniaxial tensile strength may decrease with radial compressive pressure. This conclusion is supported by present observations. According to the tensile test results, the uniaxial tensile strength for 20 mm foam is 1.31 MPa. The shear strength from the pure shear test is 0.76 MPa. A pure shear stress state is equivalent to a tensile stress in 45° of the shear direction and an equal compressive stress in its vertical direction. This means that the tensile strength of the foam reduces to 0.76 MPa due to the existence of a transverse compression.

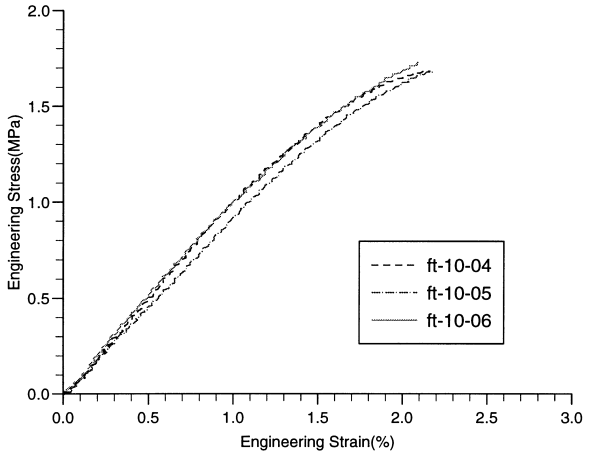

Fig. 11. Uniaxial tensile test results (three repeat tests) for 10 mm Rohacell-51WF foam.

3. Compressive-shear test

3.1. Introduction

A series of experimental and theoretical studies on the impact behaviour of polymer composite sandwich beams have been done by Mines et al. (1994), Mines and Jones (1995) and Mines (1998). It was found that the core material underneath the impact loading area is subjected to multi-axial stresses, as shown in Fig. 12, where the foam material response and failure depend on its interactive behaviour under compressive and shear stresses. Therefore, transverse shear effects on the compressive behaviour of core foam become an important issue in modelling the impact response of a sandwich beam or panel. In their elastic–plastic analysis model, Mines and Jones (1995) used a linear interaction criterion to describe shear effects on compressive yielding, i.e.,

$$\frac{\sigma}{\sigma_y} + \frac{\tau}{\tau_f} = 1 \tag{5}$$

where σ_y is the yield or plateau stress from an uniaxial compression test, and τ_f is the shear failure stress. No experimental verification was made on this assumption in Mines and Jones (1995).

In order to verify this assumption, a compressive-shear test rig is designed to examine shear effects on the compressive behaviour of Rohacell-51WF rigid, closed-cell foam, which will be described in Section 3.2.

3.2. Experimental description

A symmetric specimen block is designed for this test. Four identical foam specimens are glued on to steel plates. The layout of the compressive-shear test rig is shown in Fig. 13, in which the test block is placed on the bottom loading plate of INSTRON machine. Constant transverse force, which is monitored by a load cell-amplifier system, is applied to two middle plates to supply transverse shear force on the foam specimens. This force is supplied by a piston using high pressure gas from an air compressor. The air pressure can be adjusted to give a constant force through a valve. A rigid frame is used around the specimen block for supplying transverse tension force. The complete testing rig is hung on the INSTRON beam by a constant force spring to allow it to move in the vertical direction freely without influencing the transverse and compressive force applied on specimens in the test block. The photograph of the actual test rig is shown in Fig. 14.

The test block has two layers. Each layer consists of two specimens, as shown in Fig. 13. The

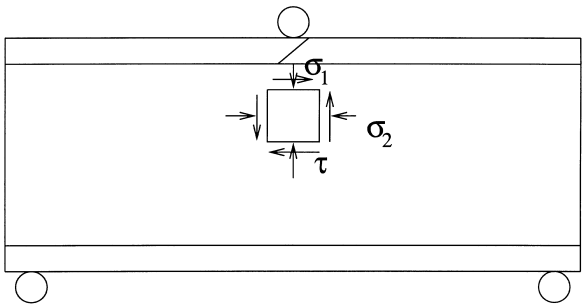

Fig. 12. Multi-axial stress state in core material of sandwich panel when subjected to three point bend.

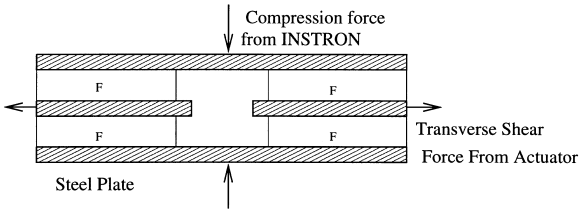

Fig. 13. Layout of the compressive shear test rig (F : foam specimens).

transverse force applied on the steel plate between two layers supplies the transverse shear force to the specimen. The dimensions of specimens are $20 \times 20 \times 10$ mm.

Experiments were conducted on a standard INSTRON 50 kN servo-hydraulic machine. The compressive loading rate was 1 mm/min, which gives a nominal engineering compressive strain rate of 8.3×10^{-4} s^{-1} in the foam specimen. The compressive displacement from the cross-head and the compressive force from the load cell are recorded to calculate engineering stress and strain.

3.3. Experimental results

The engineering stress–strain curves for the tested specimens are plotted in Fig. 15, from which the plateau stresses are determined corresponding to different transverse shear stresses. Table 6 gives the

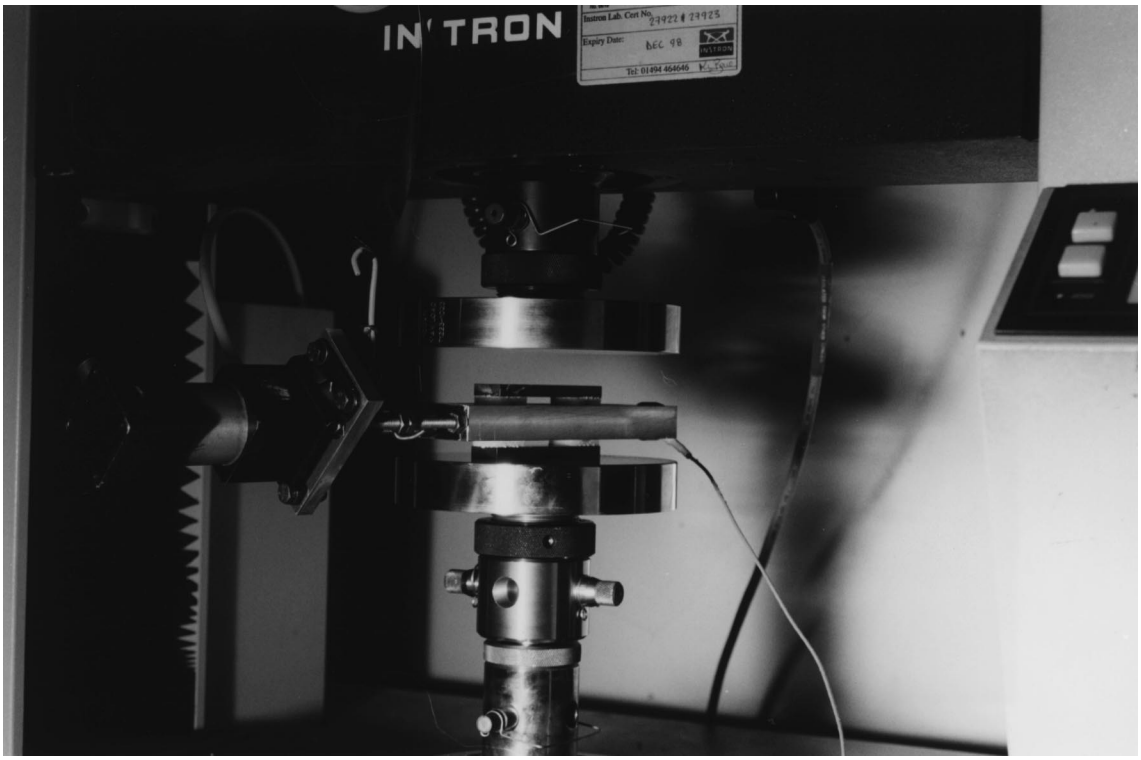

Fig. 14. Photograph of the compressive shear test rig in INSTRON test machine.

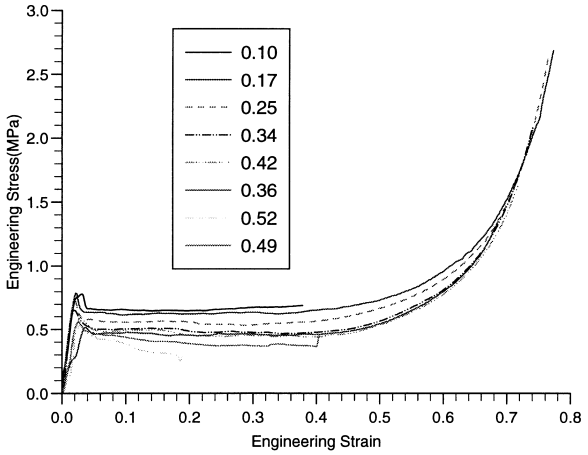

Fig. 15. Compressive stress–strain results of foam specimen under various constant shear stress ratios, τ/τ_f, shown in the figure.

actual measured values. Fig. 15 indicates that the plateau stress decreases with increased transverse shear stress. The relationships between dimensionless plateau stresses and dimensionless transverse shear stresses are plotted in Fig. 16, which shows that a linear relationship, given by Eq. (5) from Mines and Jones (1995), can describe the transverse shear effects on the plateau stress. It should be noted that the core material described in Mines and Jones (1995) has high density and has some strain hardening in uniaxial compression.

The deformation in the vertical direction is in the form of a progressive propagation process, normally initiated from the upper boundary of specimen. As soon as the first cell layer of the foam begins to crush, all plastic deformations are localised into this layer. The crush force is fairly constant during the subsequent crush process of this layer. However, when the cells in this layer start to compact, or start to lock-up, the crushed layer tends to offer a higher stress as the deformation still carries on, and this triggers another layer to start crushing. The newly crushed cell layer will repeat the same process of the previously crushed layer until all the foam layers are ready to lock-up. This feature is the same as in uniaxial compressive test, as shown by Li and Mines (1999). The specimen deformations in the horizontal direction are uniform during the early loading stage. Thus, the engineering plateau stress

Table 6
Variations of yield (plateau) stresses with transverse shear stress

No.	τ (MPa)	τ/τ_f	σ (MPa)	σ/σ_y
Compressive	0.0	0.0	0.80	1.0
MAC-10-1	0.076	0.10	0.66	0.83
MAC-10-2	0.13	0.17	0.64	0.80
MAC-10-3	0.19	0.25	0.58	0.72
MAC-10-4	0.26	0.34	0.50	0.62
MAC-10-5	0.32	0.42	0.48	0.60
MAC-10-6	0.27	0.36	0.47	0.58
MAC-10-9	0.40	0.52	0.42	0.52
MAC-10-11	0.37	0.49	0.45	0.56
Pure Shear	0.76	1.0	0.00	0.0

and engineering strain obtained by using total compressive force and displacement during the early response stage is independent of the foam geometry, and thus, can be considered as a material property. With the further development of compressive deformation, deformations in the horizontal direction in each specimen become non-uniform, especially in the region of two outside edges where a tension region and a compression region will developed, as shown in the tested specimen (Fig. 17). In most cases, tension failure is observed in the tension region. It is evident that the deformation and stress distributions in the specimen are not uniform during the later stage of deformation. The stress and strain obtained from total force and displacement are structural responses, which cannot be used to obtain material parameters when the deformation distributions are not uniform. However, this information can be used as structural response under given boundary conditions to verify FE simulation results. It should be noted that the final deformations of the four specimens are fairly identical for each test, which proves that the current test design is reliable.

All tests with transverse shear stress below 0.32 MPa kept integrity after test, although a tension crack is found within the tension zone. However, all tests with transverse shear stress larger than 0.37 MPa failed completely soon after the compressive force is applied. The test results of specimen MAC-10-9, shown in Fig. 18, belongs to this case. It should be noted that pure shear tests were conducted using the current rig up to a transverse shear stress of 0.68 MPa without failure. No more tests were done for higher transverse shear stress due to the limitations of the test set up. But, it is believed that the maximum transverse shear stress in the current test is similar to the value obtained from pure shear test (i.e., 0.76 MPa in Section 2.4).

Fig. 15 shows that, at large strains, the compression stress–strain curves for different amounts of shear tend to the same curve. In other words, the crush behaviour of the foam at densification is independent of the level of applied shear.

4. Influence of crushing damage on tensile strength

Low density foam material may be damaged easily due to accidental mass impact, which may

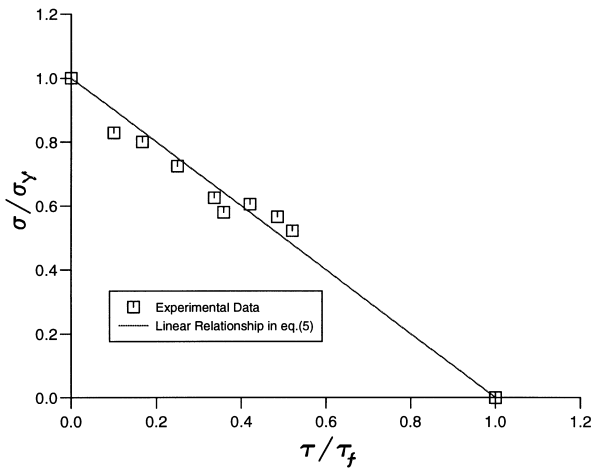

Fig. 16. Relationships between non-dimensional compressive stress (σ/σ_y) and shear stress (τ/τ_f) according to Table 6.

influence its strength in tension or shear. Tensile tests on pre-compressed foam specimens were conducted to study the influence of compressive crushing damage on tensile behaviours.

Fig. 19 gives the tensile stress–strain curves for the pre-compressed foam specimens. The information on pre-compressed specimens is given in Table 7. Three distinguishing facts are observed, i.e., (1) the form of the tensile stress–strain curve with pre-compression is similar to the compressive stress–strain curve, but having a lower plateau stress; (2) there is a remarkable decrease of tensile strength for pre-compressed specimens; (3) there is a remarkable increase of material ductility depending on the pre-compressive strain. Both the "tensile plateau stress" and tensile strength are independent of the pre-compression strain within the test range of 0.25–0.85 pre-compressive strain. The averaged values of tensile plateau stress and tensile strength for pre-compressed foam specimens are 0.15 and 0.46 MPa, respectively. The tensile strength of the damaged foam reduces to about one third of the undamaged foam. It is evident that the compressive damage will lead to a great influence on mechanical properties of the foam. However, this fact is hardly considered in previous foam material models. Thus, further studies are necessary to explore damage effects on foam behaviours.

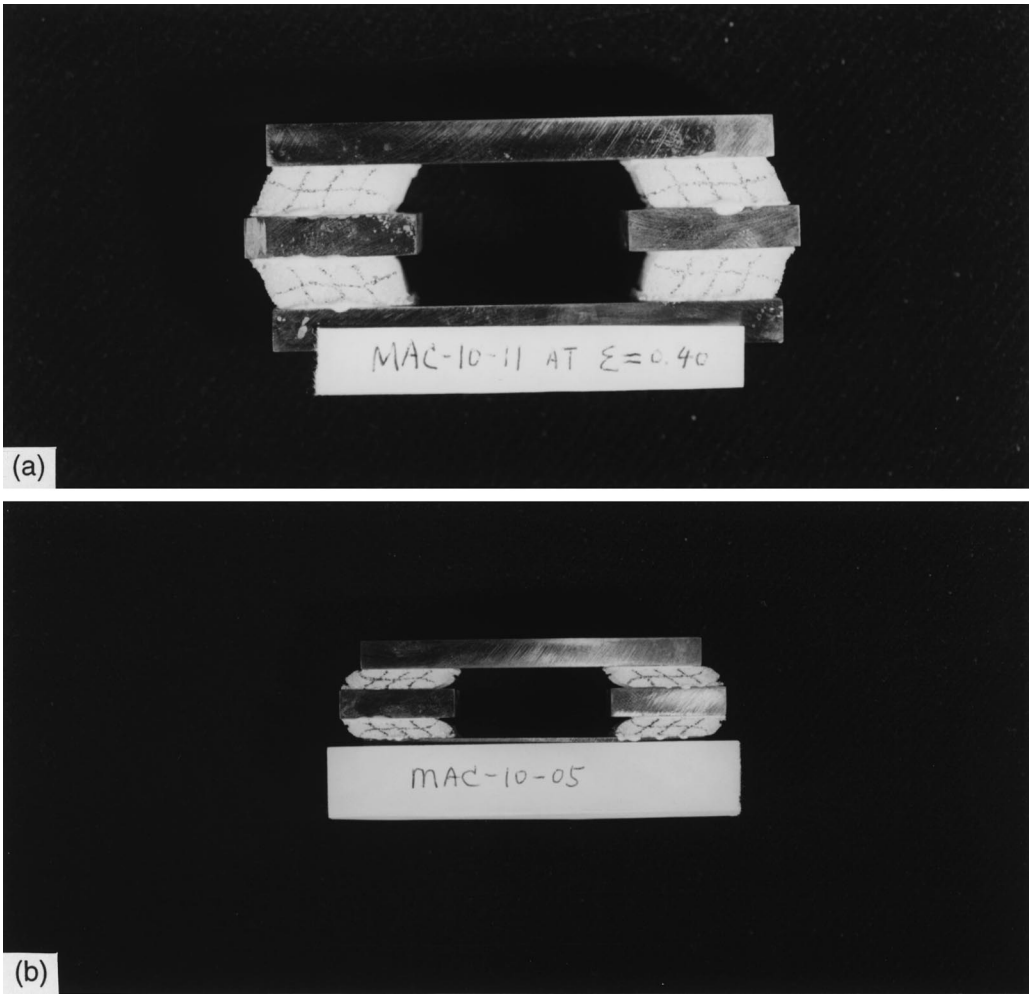

Fig. 17. Final deformation of the tested specimen: (a) at 0.4 compressive strain and (b) at 0.75 compressive strain.

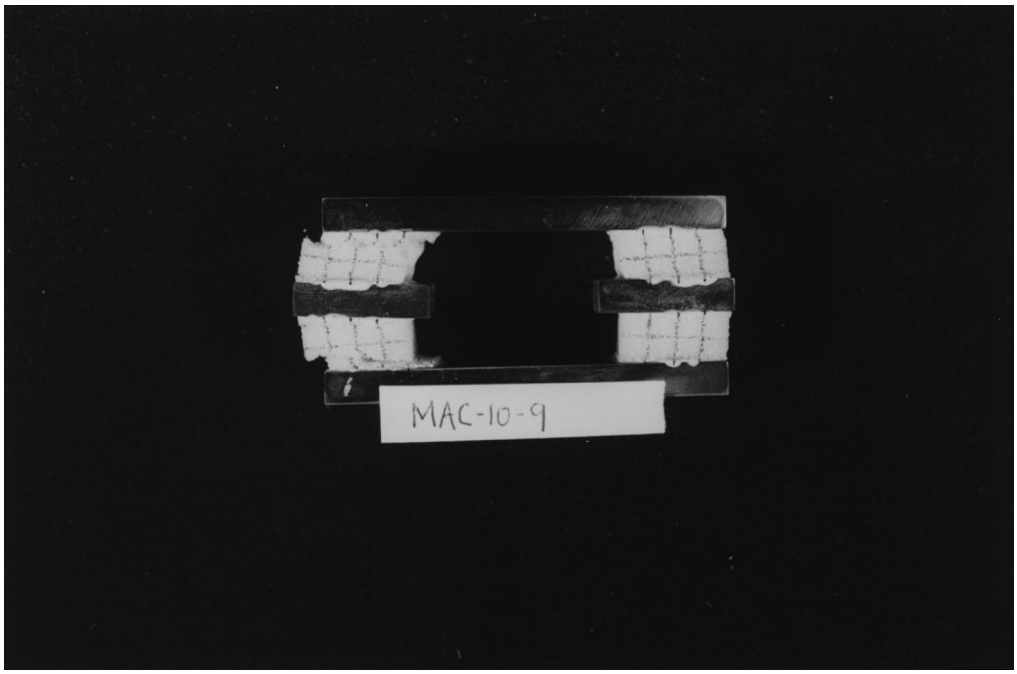

Fig. 18. Failure mode in compressive shear test with $\tau/\tau_f = 0.52$ (or, $\tau = 0.40$ MPa).

5. Discussion

According to the experimental results in uniaxial tension and compression, pure shear and hydrostatic compression, the details of the foam failure locus in plane stress space are presented for Rohacell-51WF foam in Fig. 20. Point A corresponds to hydrostatic compression, Point B to uniaxial compression, Point C to pure shear, and Point D to uniaxial tension. It should be noted that Points C and D are

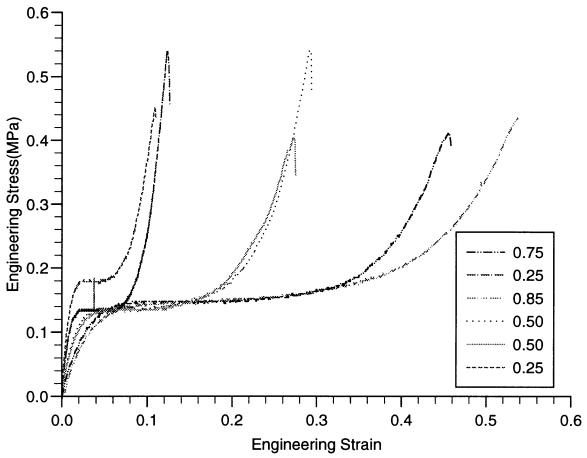

Fig. 19. Uniaxial tensile test results for the pre-compressed foams (pre-compressive strains are shown in the figure).

Table 7
Tensile tests on pre-compressed foam material (foam thickness = 20 mm)[a]

No.	Pre-strain	ε^e	ε^p
CT-1T	0.75	0.20	0.55
CT-2T	0.25	0.09	0.16
CT-3T	0.85	0.20	0.65
CT-4T	0.50	0.15	0.35
CT-5T	0.50	0.15	0.35
CT-6T	0.25	0.09	0.16

[a] Pre-strain: pre-compressive strain; ε^e: recoverable pre-compressive strain; ε^p: unrecoverable pre-compressive strain.

associated with foam tension fracture and the plastic flow model of foam material described at the end of this section is not valid in the tension stress domain range corresponding to C-D-D-C in Fig. 20. Also, it should be noted that the stress state for point A is tri-axial whereas, the stress states for points B, C and D are not.

Within the initial yielding surface, foam responses elastically. Strictly speaking, the elastic response of foam material cannot be simplified into isotropic linear elasticity. Non-linearity, anisotropy and visco-elasticity are the most obvious features of the studied foam. Some of these features have been discussed in Li and Mines (1999). Because the main application of foam material is for energy absorption, foam responses under considerable compression have been studied intensively, where the elastic response is thought to have negligible effects on compressive responses and energy absorbing capabilities of a foam. However, a recent study on strain measurement in Rohacell-51WF foam in uniaxial compression indicates that elastic strain might be as high as 12% of the total strain at $\varepsilon = 69.0\%$ during compression (Li and Mines, 1999). Also, the compressive Young's modulus decreases with increase of strain, which has been observed by Donald and Maji (1992) and illustrated by Li and Mines (1999). These observations suggest that the effects of the elastic deformation in analysing crushable foam might need to be considered in some cases for more realistic predictions.

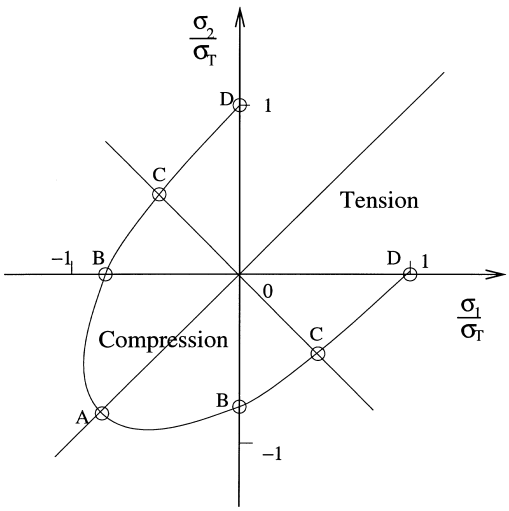

Fig. 20. Yield stress locus of Rohacell-51WF foam in plane stress state, σ_T: tensile stress at failure.

According to the present results, the average yield stress in uniaxial compression is 0.8 MPa. The hydrostatic compressive yield pressure is 0.82 MPa, which is very close to the uniaxial compression yield stress. This suggests that the principal compressive stress might control the compression yielding in the present foam. Similar observations were reported by Shaw and Sata (1966), Patel and Finnie (1969) and Zaslawsky (1973), and this behaviour is classified as a maximum principal stress criterion (Triantafillou et al., 1989). This criterion is supported by the present experimental results in the compressive–compressive range. It has been shown that foam experiences little plastic deformation in the pure shear test before the complete failure is initiated, which is distinguished from the large plastic deformations due to the core crush in compressive–compressive range. Thus, it is necessary to use different material constitutive models and failure criteria in these two ranges in principal stress space.

The theory of the micro-mechanics of cellular materials has been developed by Gibson and Ashby (1988) and Chen and Lakes (1995). The latter authors developed a micro-mechanics model for Rohacell closed-cell foams based on the tetrakaidecahedral unit cell shape, which predicts

$$\frac{E}{E_s} = \frac{0.343 + 0.823\dfrac{\rho^*}{\rho_s}}{0.684 + \dfrac{\rho^*}{\rho_s}} \frac{\rho^*}{\rho_s} \tag{6a}$$

and

$$\frac{\sigma_{pl}}{\sigma_{ys}} = 0.454\left(0.417 + \frac{\rho^*}{\rho_s}\right)\frac{\rho^*}{\rho_s} \tag{6b}$$

where the geometric relationship for closed cell foam (Gibson and Ashby, 1988)

$$\frac{\rho^*}{\rho_s} = 1.18\frac{t}{l} \tag{7}$$

is used, where l and t are the characteristic cell-wall size and thickness given in Section 2.1, E and E_s are Young's modulus of foam and cell-wall material, respectively, and σ_{pl} and σ_{ys} are the compressive crushing stress of the foam and the yield stress of the cell-wall material, respectively, which have been presented in Tables 2, 3 and 5. It should be noted that Eq. (18) in Chen and Lakes (1995) should be corrected to Eq. (6b) in the present paper. As shown in Table 8, experimental results for uniaxial behaviour agree well with predictions based on Eq. (6) and (7).

For most low density foams, the mechanical behaviour in the tension stress range is quite different from the behaviour in the compressive stress range. Most existing foam material models are only suitable in the compressive stress domain range. This can already meet requirements for some applications where the crushable foam is used in compressive stress domain range. However, when a complex stress state is involved, shear compressive and shear tensile stress states may exist, which require the foam model to be generally valid in both tensile and compressive domain ranges. The difficulties to obtain a general foam model are due to the different deformation and

Table 8
Comparison between micro-mechanics prediction and experimental results

ρ^*/ρ_s (Table 2)	ρ^*/ρ_s (Eq. (7))	E/E_s (Tables 2 and 5)	E/E_s (Eq. (6a))	σ_y/σ_{ys} (Table 2 and 3)	σ_{pl}/σ_{ys} (Eq. (6b))
0.043	0.047	0.017	0.022	0.0089	0.0083

failure mechanisms in tensile domain and compressive domain ranges. Both experimental studies and analyses based on microscopic mechanics are necessary for approaching a realistic foam model.

Strain rate effects on foam response and failure under compressive and pure shear tests have been presented in the paper. Strain rate dependence of foam material is essential for modelling the dynamic crushing process of foam materials. Some work has been done to explore the expressions for strain rate dependence for various foam materials (Nagy et al., 1964; Ramon et al., 1990; Sherwood and Frost, 1992; Zhang et al., 1997). An empirical equation, Eq. (1), is given here to describe the strain rate dependency of compressive yield stress within strain rate range of 10^{-4} to 10^{2} s^{-1}. The strain rate dependencies of compressive lock-up strain, shear failure stress and strain are also discussed. Generally, compressive yield stress increases with increase of strain rate up to 10^{0} s^{-1}, which agrees with conclusions for other foams (Ramon et al., 1990; Sherwood and Frost, 1992; Zhang et al., 1997). However, the compressive yield stress is independent of strain rate from 10^{0} to 10^{2} s^{-1} for Rohacell-51WF foam, which has not been observed for other foams.

Another important environmental factor to influence the mechanical behaviour of foam material is temperature. Sherwood and Frost (1992) and Zhang et al. (1997) showed an obvious temperature dependency of polymeric foams from -20° to 80°C under uniaxial compression, which indicated a significant decrease of compressive stress with increase of temperature. Temperature effects were not studied in the present paper, where all tests were conducted at room temperature.

Rohacell foam has low density and fails in tension in a brittle manner. The experimental techniques developed in the paper have been used to measure the properties of higher density and more ductile foams viz. Divinycell H100 and H200 (Alias and Mines, 1998) and Airex C70-200 (Mines et al., 1998).

The primary motivation of the present work was to provide necessary experimental results on material properties for the foam material model in a finite element simulation. Bilkhu et al. (1993) described the material model input requirements for two standard commercial finite element codes, ABAQUS and DYNA-3D. The material data input for crushable foam model in ABAQUS will be discussed briefly in the present paper.

The crushable foam model in ABAQUS is based on critical state theory with modifications specific to foams viz. volumetric deformation effects and non-associated flow rule (HKS Inc, 1998). The flow potential in the ABAQUS crushable foam model is based on simple laboratory experiments performed by Bilkhu (HKS Inc, 1998), which suggested that loading in any principal direction causes insignificant deformations in the other directions. A brief proof was given by Zhang et al. (1997).

The following inputs are required by the ABAQUS crushable foam model

1. uniaxial compressive failure stress, σ_0;
2. hydrostatic compressive failure stress, P_c;
3. hydrostatic tensile strength, P_t;
4. strain hardening data from the hydrostatic compressive test;
5. material parameter K restricted by $0.778 \leq K \leq 1.0$.

When $K = 1.0$, the failure surface does not depend on the third deviatoric stress invariant, which has been used by Zhang et al. (1997) to implement the crush model in DYNA-3D to simulate the indentation test of polymeric foams. However, Zhang et al. (1997) used σ_0, P_c and the shear yielding stress, τ_0, to determine the failure surface instead of σ_0, P_c and P_t in the ABAQUS crushable foam model.

ABAQUS assumes that P_t equals 10% of P_c, which does not agree with experimental evidence observed in the present paper. Hydrostatic tensile tests have not been conducted here as they are very difficult to undertake in practice. Normally, P_t is larger than the uniaxial tensile strength (Gibson and Ashby, 1988). Therefore, in the present case, P_t is larger than P_c and $P_t = 0.1\,P_c$ will lead to a concave failure

surface. However, if one realises that the crushable foam model is only applicable for the compressive stress domain range, the influence of P_t on the failure surface in the compressive stress domain range is not significant within a wide variation of P_t.

It should be noted that finite element analysis assumes a constant or linear distribution of strain components within an element, whereas, localised deformation is a characteristic of Rohacell-51WF foam. Further discussion on this issue is given in Li and Mines (1999).

6. Conclusions

Mechanical behaviours of Rohacell-51WF rigid crushable foam are studied in the present paper. Basic mechanical properties in uniaxial tension and compression and pure shear are obtained using existing test standards. A hydrostatic compressive test rig is designed in order to obtain foam properties under hydrostatic pressure. These results offer basic mechanical properties of foam material, required in most of the foam material models for FE simulation. However, the mechanical behaviours of cellular foam materials are much more complicated than solid materials due to the cellular nature of the foam structure. Foam responds very differently in the compressive domain as compared with the tensile domain stress states due to different deformation and failure mechanisms. Compressive damage effects on the tensile properties are also addressed. Although not considered here, foam anisotropy has been identified as an important aspect for further study.

A test rig is developed in the paper to study the foam response under multi-axial stress state. In the present case, the compressive responses of Rohacell-51WF foam under various transverse shear forces are reported. Experimental results show that compressive yielding/plateau stress decreases with an increase of transverse shear stress, which can be described by a linear relationship between the dimensionless compressive failure/plateau stress and dimensionless shear stress. The compressive deformation process of the specimen subjected to constant transverse force is described and discussed.

The material test results can be used to determine parameters in material models and the compressive shear results may be used to examine the validity of material models through the FE method.

Acknowledgements

This research is supported by 'CRASURV — Design For Crash Survivability of Commercial Aircraft' which is a RTD project partially funded by the European Union under the Aeronautics Area of the programme on Industrial and Material Technology (BRITE/EURAM). Experiments were conducted in the Impact Research Centre in the University of Liverpool. Dr. J.A. Close assisted in the initial foam tests.

References

Akay, M., Hanna, R., 1990. A comparison of honeycomb-core and foam-core carbon-fibre/epoxy sandwich panels. Composites 21, 325–331.

Akfert, A., 1994. Finite element analysis of composite sandwich beams and panels. M.Sc. Thesis, University of Manchester Institute of Science and Technology.

Alias, A., Mines, R.A.W., 1998. Experimental results and techniques on the crush behaviour of structural foams. In: Third Int. Symposium on Impact Engng., Singapore.

ASTM C273-61, Standard test method for shear properties in flatwise plane of flat sandwich constructions or sandwich cores.

ASTM C297-61, 1984. Standard method of tensile test of flat sandwich constructions in flatwise plane.

ASTM C365-57, Standard test methods for flatwise compressive strength of sandwich cores.
ASTM D3574-91, Standard test methods for flexible cellular material-slab, bonded, and molded Urethane foams.
Bernard, M.L, Lagace, P.A., 1987. Impact resistance of composite sandwich plates. In: Proceedings of the American Society for Composites, 2nd Tech. Conf., Tech. Pub. Co. Inc., 167–176.
Bilkhu, S.S., Founas, M., Nusholtz, G.S., 1993. Material modeling of structural foams in finite element analysis using compressive uniaxial and triaxial data. In: International Cong. and Exposition, Detroit, MI, SAE Technical Paper Series 930434.
Chen, C.P., Anderson, W.B., Lakes, R.S., 1994. Relating the properties of foam to the properties of the solid from which it is made. Cellular Polymers 13, 16–32.
Chen, C.P., Lakes, R.S., 1995. Analysis of the structure–property relations of foam materials. Cellular Polymers 14, 186–202.
Donald, S., Maji, A.K., 1992. Contractor's Reports 54-5043 to Sandia National Laboratories, Albuquerque, NM.
Gibson, L.J., Ashby, M.F., 1988. Cellular Solids. Pergamon Press, Oxford.
HKS Inc., 1998, ABAQUS Theory Manual, Version V5.6.
Li, Q.M., Mines, R.A.W., 1999. Strain localization in rigid crushable foam during uniaxial compression, University of Liverpool, Impact Research Centre Report No. IRC/183/99.
Maji, A.K., Schreyer, H.L., Donald, S., Zuo, Q., Satpathi, D., 1995. Mechanical properties of polyurethane foam impact limiters. ASCE J. of Engng. Mech 121, 528–540.
Mines, R.A.W., Worrall, C.M., Gibson, A.G., 1994. The static and impact behaviour of polymer composite sandwich beams. Composites 25 (2), 95–110.
Mines, R.A.W., Jones, N., 1995. Approximate elastic–plastic analysis of the static and impact behaviour of polymer composite sandwich beams. Composites 26 (12), 803–814.
Mines, R.A.W., 1998. Impact energy absorption of polymer composite sandwich beams. Key Engng. Materials 141-143, 553–572.
Mines, R.A.W., Li, Q.M., Alias, A., Birch, R.S., Close, J.A., 1998. On the measurement of the crush behaviour of structural foams. In: Allison, I.M. (Ed.), Proceedings of the 11th Int. Conf. on Exp. Mech., Oxford, pp. 287–292.
Neilsen, M.K., Krieg, R.D., Schreyer, H.L., 1995. A constitutive theory for rigid polyurethane foam. Polymer Engng. and Science 35, 387–394.
Nagy, A., Ko, W.L., Lindholm, U.S., 1964. Mechanical behaviour of foamed materials under dynamic compression. J. of Cellular Plastics 10, 127–134.
Patel, N.R., Finnie, I., 1969. Report UCRL-13420, Lawrence Livermore Laboratory, Livermore, CA.
Ramon, O., Mizrahi, S., Miltz, J., 1990. Mechanical properties and behaviour of open-cell foams used as cushioning materials. Polymer Engng. and Science 30, 197–201.
Roehm, 1998. Rohacell WF PMI foam, Roehm Ltd., Bradbourne Drive, Tilbrook, Milton Keynes, Bucks, MK7 8AU.
Shaw, M.C., Sata, T., 1966. The plastic behaviour of cellular materials. Int. J. Mech. Sci 8, 469–478.
Sherwood, J.A., Frost, C.C., 1992. Constitutive modeling and simulation of energy absorbing polyurethane foam under impact loading. Polymer Engng. and Science 32, 1138–1146.
Theocaris, P.S., 1992. Failure modes of closed-cell polyurethane foams. Int. J. of Fracture 56, 353–375.
Triantafillou, T.C., Zhang, J., Shercliff, T.L., Gibson, L.J., Ashby, M.F., 1989. Failure surfaces for cellular materials under multiaxial loads. Part II: Comparison of models with experiment. Int. J. Mech. Sci 31, 665–678.
Triantafillou, T.C., Gibson, L.J., 1990. Constitutive modeling of elastic–plastic open-cell foams. ASCE J. of Engng. Mech 116, 2772–2778.
Tsang, P.H.W., Dugundji, J., 1990. Damage resistance of graphite/epoxy sandwich panels under low speed impacts. J. of the American Helicopter Society 37, 75–81.
Wu, C.L., Sun, C.T., 1996. Low velocity impact damage in composite sandwich beams. Composite Structures 34, 21–27.
Zaslawsky, M., 1973. Multiaxial stress studies on rigid polyurethane foam. Experimental Mechanics 13, 70–76.
Zhang, J., Lin, Z., Wong, A., Kikuchi, N., Li, V.C., Yee, A.F., Nusholtz, G.S., 1997. Constitutive modelling and material characterisation of polymeric foams. ASME J. of Eng. Matls. Tech 119, 284–291.